Original Article

JCBFM

Journal of Cerebral Blood Flow & Metabolism
2024, Vol. 44(3) 345–354

DOI: 10.1177/0271678X231212173
journals.sagepub.com/home/jcbfm
Sage

Blood-brain barrier disruption imaging in postoperative cerebral hyperperfusion syndrome using DCE-MRI

Kanghwi Lee[1], Roh-Eul Yoo[1,*], Won-Sang Cho[2,*], Seung Hong Choi[1,3,4], Sung Ho Lee[2], Kang Min Kim[2], Hyun-Seung Kang[2] and Jeong Eun Kim[2]

Abstract

Little has been reported about the association between cerebral hyperperfusion syndrome (CHS) and blood-brain barrier (BBB) disruption in human. We aimed to investigate the changes in permeability after bypass surgery in cerebrovascular steno-occlusive diseases using dynamic contrast-enhanced MRI (DCE-MRI) and to demonstrate the association between CHS and BBB disruption. This retrospective study included 36 patients (21 hemispheres in 18 CHS patients and 20 hemispheres in 18 controls) who underwent combined bypass surgery for moyamoya and atherosclerotic steno-occlusive diseases. DCE-MRI and arterial spin labeling perfusion-weighted imaging (ASL-PWI) were obtained at the baseline, postoperative state, and discharge. Perfusion and permeability parameters were calculated at the MCA territory ($CBF_{(territorial)}$, $K^{trans}_{(territorial)}$, $V_{p(territorial)}$) and focal perianastomotic area ($CBF_{(focal)}$, $K^{trans}_{(focal)}$, $V_{p(focal)}$) of operated hemispheres. As compared with the baseline, both $CBF_{(territorial)}$ and $CBF_{(focal)}$ increased in the postoperative period and decreased at discharge, corresponding well to symptoms in the CHS group. $V_{p(focal)}$ was lower in the postoperative period and at discharge, as compared with the baseline. In the control group, no parameters significantly differed among the three points. In conclusion, V_p at the focal perianastomotic area significantly decreased in patients with CHS during the postoperative period. BBB disruption may be implicated in the development of CHS after bypass surgery.

Keywords

Cerebral revascularization, cerebrovascular disorders, magnetic resonance imaging, perfusion, permeability

Received 18 April 2023; Revised 23 August 2023; Accepted 16 October 2023

Introduction

Cerebral hyperperfusion syndrome (CHS) is a clinically important and potentially preventable complication after revascularization procedures. CHS is characterized by clinical symptoms (pain, weakness, seizure, altered mentality and hemorrhage) and evidence of hyperperfusion on imaging.[1] Intracerebral hemorrhage (ICH) and cerebral edema are occasionally found on imaging.[2] The incidences of CHS are reported variously according to its definition and the type of revascularization procedures, with a pooled incidence of 4.6% for carotid artery stenting (CAS)[3] and 21.5% to 31.5% for superficial temporal artery to middle cerebral artery (STA-MCA) bypass in moyamoya disease (MMD).[4,5]

Various theories have been proposed about the pathophysiology of CHS.[1,2] The impairment of

[1]Department of Radiology, Seoul National University Hospital, Seoul National University College of Medicine, Seoul, Republic of Korea
[2]Department of Neurosurgery, Seoul National University Hospital, Seoul National University College of Medicine, Seoul, Republic of Korea
[3]Center for Nanoparticle Research, Institute for Basic Science (IBS), Seoul, Republic of Korea
[4]School of Chemical and Biological Engineering, Seoul National University, Seoul, Republic of Korea

*These authors contributed equally as co-corresponding authors.

Corresponding authors:
Roh-Eul Yoo, Department of Radiology, Seoul National University Hospital, Seoul National University College of Medicine, 101, Daehangno, Jongno-gu, Seoul 03080, Republic of Korea.
Email: roheul7@gmail.com

Won-Sang Cho, Department of Neurosurgery, Seoul National University Hospital, Seoul National University College of Medicine, 101, Daehangno, Jongno-gu, Seoul 03080, Republic of Korea.
Email: nsdrcho@gmail.com

cerebral autoregulation is among the most accepted theories. Normally, the diameter of cerebral vessels is spontaneously controlled as a response to arterial blood pressure change, in order to keep the normal cerebral blood flow (CBF). In chronically ischemic circumstances, however, autoregulation is impaired and arteries are fully dilated. Consequently, CBF around the targeted recipient artery keeps increasing after direct bypass surgery until the autoregulatory function is recovered, resulting in brain edema and even bleeding. Possible mediators of cerebral autoregulation impairment and blood-brain barrier (BBB) dysfunction are nitric oxide and other free radicals released during ischemic reperfusion. Nitric oxide induces vasodilatation and increases the permeability of cerebral vessels. Oxygen-derived free radicals can damage the tight junction and endothelium, resulting in BBB disruption. In a recent animal study using rat CHS models, BBB disruption was confirmed by extravasation of Evans blue dye and matrix metalloproteinase-9 level.[6]

Dynamic contrast-enhanced MRI (DCE-MRI) is a well-known method for assessing BBB disruption *in vivo*. Repeated acquisition of T1-weighted images after contrast injection can provide an enhancement signal as a function of time, from which quantitative parameters that represent BBB integrity — specifically, volume transfer constant (K^{trans}), fractional interstitial volume (V_e), and fractional plasma volume (V_p) — can be extracted.[7] Subtle changes in BBB permeability, as compared with normal brain tissue, have been delineated using DCE-MRI in various central nervous system diseases, including Alzheimer's disease, small vessel disease, migraine, traumatic brain injury, and demyelinating disease.[8–13] Arterial spin labeling perfusion-weighted imaging (ASL-PWI) is a noninvasive MRI technique that uses arterial protons as an endogenous contrast agent to quantify tissue blood flow.[14] ASL-PWI has been shown to be useful in demonstrating hyperperfusion in hypervascular tumors, vascular lesions, and epilepsy.[15–18]

The association of CHS and BBB disruption has been suggested and advocated with some animal studies.[6,19,20] However, little has been reported about the association in human brains *in vivo*. In this case-control study, we aimed to noninvasively investigate the changes in BBB permeability after combined bypass surgery in cerebrovascular steno-occlusive diseases and to demonstrate the association between CHS and BBB disruption using DCE-MRI.

Methods

This retrospective case-control study was approved by the institutional review board of Seoul National University Hospital, and the requirement for informed consent was waived due to the retrospective nature of the study. This study adhered to STROBE guidelines (Strengthening the Reporting of Observational Studies in Epidemiology) for cohort studies,[21] and was performed in accordance with the Declaration of Helsinki.

Patient selection

Among 46 operated hemispheres in 41 consecutive patients, who underwent combined bypass surgery for MMD, and atherosclerotic diseases such as MCA and internal carotid artery (ICA) occlusion between April 2020 and June 2022, 41 operated hemispheres in 36 patients (including 5 patients with both hemispheres operated during the study period) were finally selected from our database (Supplementary Figure 1).[22] The inclusion criteria for this study were as follows: the patients who (a) were aged 18 or more; (b) underwent combined bypass surgery for cerebrovascular steno-occlusive diseases between April 2020 and June 2022 in Seoul National University Hospital; (c) had recurrent ischemic symptoms, including transient ischemic attack and lacunar infarction, or hemorrhagic MMD; (d) had no other medical history such as significant traumatic brain injury, brain tumor, significant cerebral infarction, epilepsy, neuroinflammatory disease, cerebral metabolic disease, neurodegenerative disease, or other severe medical problems; (e) had significantly decreased basal perfusion and reservoir capacity on brain single photon emission computed tomography (SPECT) and perfusion delay on ASL-PWI, which clearly indicated the need for revascularization surgery; and (f) underwent preoperative and postoperative MR imaging including ASL-PWI and DCE-MRI.[22] The exclusion criteria were as follows: the patients who had (a) MR imaging with suboptimal image quality ($n = 2$) and (b) incomplete series of MR imaging ($n = 3$).

The patients were divided into CHS and control groups, based on clinical symptoms and imaging findings. CHS was diagnosed when transient neurological deterioration occurred after surgery and the focal hyperperfused area on ASL-PWI corresponded well to the neurological deficits, without signs of acute infarction or hemorrhage.[22,23] The presence of an unequivocal increase in CBF on postoperative ASL images (as compared with the preoperative images) was visually assessed by consensus agreement of a neuroradiologist (R.E.Y. with 11 years of experience) and a neurosurgeon (W.S.C. with 16 years of experience). For each patient, MR images were obtained at baseline (immediately before the surgery), in the postoperative period, and at discharge. MR imaging in the postoperative period was performed at the time of symptom onset for the CHS group and postoperative day 5–6

for the control group. MR images at discharge were acquired just before discharge for the control group and after considerable or complete symptom improvement for the CHS group.

Surgical procedures and perioperative management

Combined bypass surgery, consisting of direct (anastomosis between STA and cortical branch of MCA) and indirect (encephalo-duro-fascio-galeal synangiosis) bypass, was performed by a single surgeon (W.S.C.) under general anesthesia with intravenous propofol and remifentanil, as in the previously report.[22]

Antiplatelet and anticoagulants were generally discontinued before surgery, except for 5 cases (2 CHS patients [MCA occlusion, n = 1; MMD, n = 1] and 3 controls [ICA occlusion, n = 2; MMD = 1]) with clinical instability or recent infarction. During the postoperative period, patents were normohydrated and their hemoglobin levels were kept between 10 and 11 g/dL. Blood pressure was maintained at the preoperative level ±10 mmHg with a systemic blood pressure less than 140 mmHg. In cases suspected of postoperative CHS, diffusion-weighted imaging (DWI) and/or precontrast CT were first performed to rule out the possibility of hemorrhage and infarction. Diagnosis of CHS was made when hyperperfusion was identified on ASL-PWI and patients had symptoms corresponding to the areas. Seizure and involuntary movement as a symptom related to CHS were differentiated based on the electroencephalographic findings. Even after the diagnosis of CHS, general principles for patient management were identical to those in the immediate postoperative period, except that more precise management was adopted based on patients' symptoms and vital signs. Other medications such as edaravone, minocycline, steroids, or antiplatelets were not newly administered.

MRI protocol

All MR images, including DWI, susceptibility-weighted imaging (SWI), T2 fluid-attenuated inversion recovery (FLAIR), postcontrast T1 spin-echo, ASL, and DCE MR imaging, were obtained at a 3.0 T scanner (Discovery 750, GE Healthcare, Milwaukee, Wisconsin) using a 32-channel head coil. Detailed MR protocols are provided in the online supplemental methods and Supplementary Table 1.

ASL-PWI and DCE-MRI analysis

Image analysis was performed using NordicICE software (version 4.1.2; NordicNeuroLab). Permeability parameter (K^{trans}, V_p) maps were derived from DCE-MRI based on a pharmacokinetic model (Patlak model) by two reviewers (K.L. and R.E.Y. with 3 years and 11 years of experience, respectively) blinded to whether the patient belonged to the CHS or control group. For each study, the arterial input function (AIF) was obtained from the main intracranial arteries, including the MCA at the level of the circle of Willis. The baseline T1 was fixed at 1000 msec in this study.

ASL perfusion images were resampled and coregistered based on DCE parameter maps to minimize potential errors attributable to the differences in slice thickness, matrix size, and slice gap. Regions of interest were manually drawn at the MCA territory of the operated hemisphere (defined as a territorial mask) on two slices of each ASL image that best represented the MCA territory based on the Alberta Stroke Program Early CT Score (ASPECTS) (M1, M2, M3 at the level of the basal ganglia and M4, M5, M6 at the level immediately above the basal ganglia).[24] The MCA territory of the nonoperated hemisphere was also drawn for CBF normalization. The area of decreased perfusion delay, as compared with preoperative images, was identified on the perfusion delay map of postoperative ASL-PWI and defined as a focal perianastomotic area (focal mask) (Supplementary Figure 2). Subsequently, absolute CBF, K^{trans}, and V_p values were calculated at the MCA territory ($CBF_{(territorial)}$, $K^{trans}{}_{(territorial)}$, $V_{p(territorial)}$) and focal perianastomotic area ($CBF_{(focal)}$, $K^{trans}{}_{(focal)}$, $V_{p(focal)}$) of the operated hemisphere. Furthermore, the absolute CBF values at the MCA territory and the focal perianastomotic area of the operated hemispheres were normalized with respect to the nonoperated hemispheres ($nCBF_{(territorial)}$ and $nCBF_{(focal)}$). When deriving the value of each parameter, the upper and lower 5% values were trimmed to exclude outliers.

Statistical analysis

Statistical analyses were performed using MedCalc statistical software, version 11.1.1.0 (MedCalc, Mariakerke, Belgium). The data for each parameter were evaluated for normality with the Kolmogorov-Smirnov test. In all analyses, P values less than .05 were considered statistically significant. Nonparametric data are reported as the median and interquartile range (IQR, range from the 25th to the 75th percentile), and parametric data are presented as the mean ± standard deviation. Based on the results of Kolmogorov-Smirnov test, Friedman test, followed by post hoc tests with Bonferroni correction, was performed to compare CBF and permeability parameters (K^{trans} and V_p) among studies (at baseline, in the postoperative period, and at discharge) in each group. To assess the reproducibility of DCE parameters, intraclass correlation

coefficients (ICCs) were calculated for two sets of DCE parameters, which were extracted using AIFs obtained by two independent researchers (K.L. and R.E.Y. with 3 years and 11 years of experience, respectively).

Results

Patient characteristics and clinical symptoms

A total of 21 hemispheres in 18 CHS patients and 20 hemispheres in 18 controls were included in this study (Table 1). Seventeen patients in the CHS group and 13 patients in the control group were diagnosed with MMD. There were no significant differences in terms of age, sex, diagnosis, disease involvement, initial presentation, operated hemisphere, and underlying diseases between the two groups except the cerebral hemorrhage as a presenting symptom (20% in the control vs. 0% in the CHS group, $P = .05$). All the hemorrhagic presentations were associated with adult MMD.

Among the most common symptoms were motor dysphasia (57% [12/21]), sensory disturbance (57% [12/21]), and motor weakness (33.3% [7/21]), and dysarthria (24% [5/21]) (Supplementary Table 2). Subarachnoid hemorrhage was accompanied in one hemisphere (5% [1/21]) during the operation. The median time of symptom onset was 4 days after the operation (IQR, 3–6 days), and mild residual symptoms were present at discharge after 43% (9/21) of the operations. The median duration of symptoms (from symptom onset to considerable recovery with minimal functional impairment) was 6 days (IQR, 5-11 days).

Table 1. Clinical characteristics of CHS patients and controls.

	CHS	Controls	*P* Value
Hemispheres/patients	21/18	20/18	NA
Age (y)	45 (32–52)	42 (36–53)	.87
Sex			1.00
Male	3 (17)	4 (22)	
Female	15 (83)	14 (78)	
Diagnosis			.13
MMD	17 (94)	13 (72)	
ICAO	0 (0)	3 (17)	
MCAO	1 (6)	2 (11)	
Disease involvement			.34
Unilateral hemisphere	1 (6)	4 (22)	
Bilateral hemispheres	17 (94)	14 (78)	
Initial presentation[a]			
Cerebral ischemia			
Infarction	15 (71)	16 (80)	.72
Transient ischemic attack	19 (90)	13 (65)	.07
Cerebral hemorrhage	0 (0)	4 (20)	.05
Operated hemisphere[a]			.22
Right	8 (38)	12 (60)	
Left	13 (62)	8 (40)	
Underlying diseases			
Hypertension	4 (22)	8 (44)	.29
Dyslipidemia	7 (39)	4 (22)	.47
Diabetes mellitus	3 (17)	4 (22)	1.00

CHS: cerebral hyperperfusion syndrome; ICAO: internal carotid artery occlusion; MCAO: middle cerebral artery occlusion; MMD: moyamoya disease; NA: not applicable.

Data are number of patients (%) and medians (interquartile range) for continuous variables.

[a]Number of symptomatic hemispheres (%).

Postoperative complications included minor cerebral infarction in 1 hemisphere, intracerebral hemorrhage in 2 hemispheres (minor hemorrhage due to hemorrhagic transformation of a previous infarction [n = 1] and major hemorrhage due to the use of anticoagulants for the treatment of pulmonary thromboembolism [PTE] [n = 1]), and PTE in 1 hemisphere. The mortality rate was 0%, and the permanent morbidity rate was 2% (1/41 operations; 1 with postoperative PTE and anticoagulant-related complications including ischemic colitis and intracerebral hemorrhage). The transient morbidity rate was 5% (2/41 operations; 1 with minor cerebral infarction and 1 with minor hemorrhage due to hemorrhagic transformation of a previous infarction).

ASL and DCE MR imaging findings

MR imaging in the postoperative period was performed on a median postoperative day 4 (IQR, postoperative day 4–6) for the CHS group and on a median postoperative day 6 (IQR, postoperative day 5–6) for the control. MR images at discharge were acquired on a median postoperative day 12 (IQR, postoperative day 10–13) for the CHS group and on a median postoperative day 11 (IQR, postoperative day 10–11) for the control. Changes in CBF, K^{trans}, and V_p after combined bypass in CHS and control groups are summarized in Table 2, Supplementary Table 3, and Supplementary Table 4.

CHS group. Both $CBF_{(focal)}$ (Figures 1 and 2, Table 2) and $CBF_{(territorial)}$ (Supplementary Table 3) on the operated hemispheres increased in the postoperative period and decreased at discharge. In the pairwise comparison, $CBF_{(focal)}$ showed differences in values at baseline vs. in the postoperative period (median, 76.3 vs. 122.1 mL/100 g/min; $P < .001$, respectively), in the postoperative period vs. at discharge (median, 122.1 vs. 96.1 mL/100 g/min; $P < .001$), and at baseline vs. at discharge (median, 76.3 vs. 96.1 mL/100 g/min; $P = .02$). Similarly, $CBF_{(territorial)}$ showed differences in values at baseline vs. in the postoperative period (median, 80.5 vs. 98.4 mL/100 g/min; $P < .001$, respectively), in the postoperative period vs. at discharge (median, 98.4 vs. 93.0 mL/100 g/min; $P = .005$), and at

Table 2. Difference in CBF, K^{trans} and V_p in focal masks of the operated hemispheres between imaging times.

Group	Parameter	Imaging time	Value (Interquartile range)	*P* Value[a]	Imaging time (*P Value*)[b]	
					Postop.	Discharge
CHS	CBF (mL/100 g/min)	Baseline	76.3 (57.9–101.2)	<.001	<.001	.02
		Postop.	122.1 (99.6–132.4)		...	<.001
		Discharge	96.1 (82.0–108.2)		...	...
	nCBF	Baseline	0.957 (0.754–1.15)	<.001	.002	.24
		Postop.	1.218 (1.083–1.356)		...	.008
		Discharge	1.050 (0.979–1.166)		...	...
	K^{trans} (min^{-1})	Baseline	0.00134 (0.00082–0.00207)	.41	.87	.34
		Postop.	0.00120 (0.00079–0.00167)		...	>.99
		Discharge	0.00116 (0.00067–0.00134)		...	...
	V_p	Baseline	3.54 (2.48–4.90)	.01	.04	.02
		Postop.	2.63 (2.24–3.81)		...	>.99
		Discharge	2.80 (1.87–4.14)		...	...
Control	CBF (mL/100 g/min)	Baseline	71.1 (59.9–92.4)	.02	.29	>.99
		Postop.	87.0 (74.7–99.3)		...	.16
		Discharge	74.0 (66.6–84.8)		...	...
	nCBF	Baseline	1.031 (0.873–1.102)	.36	.53	.46
		Postop.	1.034 (0.907–1.224)		...	>.99
		Discharge	1.073 (0.848–1.182)		...	...
	K^{trans} (min^{-1})	Baseline	0.00151 (0.00108–0.00217)	.14	.07	.50
		Postop.	0.00131 (0.00061–0.00186)		...	>.99
		Discharge	0.00104 (0.00047–0.00152)		...	...
	V_p	Baseline	3.49 (2.74–4.79)	.27	.10	.65
		Postop.	3.20 (2.22–4.49)		...	>.99
		Discharge	3.23 (2.20–5.02)		...	...

CBF: cerebral blood flow; nCBF: normalized cerebral blood flow.
[a]Friedman test.
[b]Wilcoxon test, *P* values were adjusted for multiple comparisons with the use of Bonferroni correction (n = 3).

baseline vs. at discharge (median, 80.5 vs. 93.0 mL/100 g/min; $P = .04$). $nCBF_{(focal)}$ showed differences in values at baseline vs. in the postoperative period (median, 0.957 vs. 1.218; $P = .002$, respectively) and in the postoperative period vs. at discharge (median, 1.218 vs. 1.05; $P = .008$) (Table 2). $V_{p(focal)}$ was lower in the postoperative period (median, 2.63) and at discharge (median, 2.80), as compared with baseline (median, 3.54) ($P = .04$ and $P = .02$, respectively) (Figures 1 and 2, Table 2). $V_{p(territorial)}$ did not show a significant difference among the three time points ($P = .27$) (Supplementary Table 3). $K^{trans}_{(focal)}$ and $K^{trans}_{(territorial)}$ did not significantly differ among the three time points ($P = .41$ and $P = .55$, respectively) (Table 2 and Supplementary Table 3). On the nonoperated hemispheres, $CBF_{(territorial)}$ increased in the postoperative period (median, 83.0 vs. 88.8 mL/100 g/min; $P = .009$) and decreased at discharge (median, 88.8 vs. 87.0; $P = .01$) (Supplementary Table 4). $V_{p(territorial)}$ and $K^{trans}_{(territorial)}$ did not show any significant change among the three time points ($P = .55$ and $P = .38$, respectively).

Control group. CBF, K^{trans} and V_p values on the operated hemispheres were not significantly different among the three time points (all $Ps > .05$) (Figures 1 and 3, Table 2 and Supplementary Table 3). $CBF_{(territorial)}$ on the nonoperated hemisphere mildly increased in the postoperative period and decreased at discharge (Supplementary Table 4). In the pairwise comparison, $CBF_{(territorial)}$ on the nonoperated hemisphere showed a difference in values in the postoperative period vs. at discharge (median, 87.5 vs. 77.4 mL/100 g/min; $P = .006$, respectively). $V_{p(territorial)}$ and $K^{trans}_{(territorial)}$ did not significantly differ among the three time points ($P = .72$ and $P = .25$, respectively) (Supplementary Table 4).

Interobserver agreements for DCE-MRI parameters

ICCs for mean K^{trans} and V_p were 0.70 (95% CI: 0.11, 0.87) and 0.90 (95% CI: 0.86, 0.93) in the focal mask, indicating substantial and almost perfect agreement, respectively. In the territorial mask, ICCs for mean K^{trans} and V_p were 0.45 (95% CI: 0, 0.68) and 0.81 (95% CI: 0.73, 0.87), indicating moderate and almost perfect agreement, respectively.

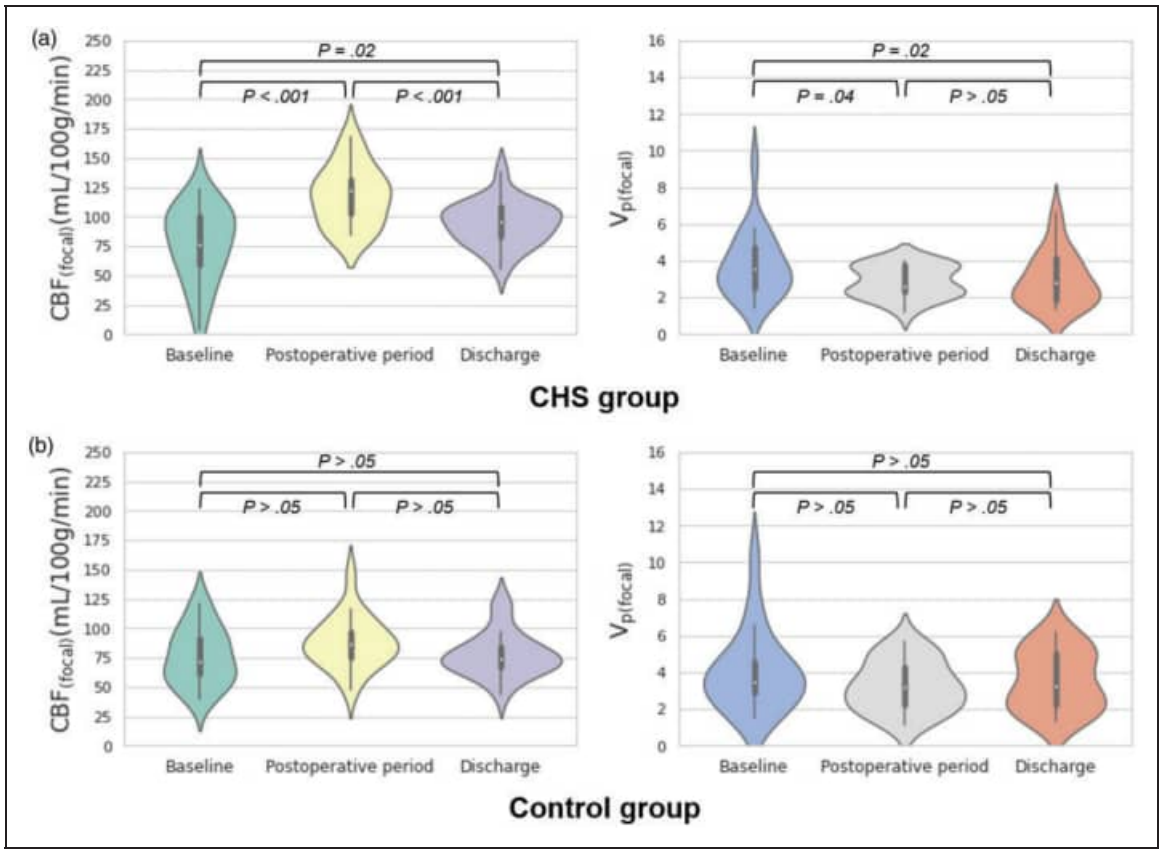

Figure 1. Violin plots of $CBF_{(focal)}$ and $V_{p(focal)}$ changes in CHS and control groups. Violin plots of CBF and V_p in the perianastomotic area at three time points (baseline, postoperative period, discharge) are shown for the CHS (a) and control (b) groups. Inner box-and-whisker plots represent the following: white points = median, boundaries of boxes = 25th to 75th percentile range, whiskers = 25th percentile − 1.5 interquartile range to 75th percentile + 1.5 interquartile range. $CBF_{(focal)}$, cerebral blood flow in the focal perianastomotic area; CHS, cerebral hyperperfusion syndrome; $V_{p(focal)}$, fractional plasma volume in the focal perianastomotic area.

Discussion

The association of BBB disruption and CHS has been proposed, but *in vivo* data from the human brain remain scarce.[6,25] We investigated the changes in BBB permeability and cerebral perfusion after combined bypass surgery in patients with cerebrovascular steno-occlusive diseases using DCE-MRI and ASL-PWI. Key findings were as follows: (a) In the CHS group, CBF at the focal perianastomotic area increased in the postoperative period with development of the corresponding symptoms, and decreased at discharge; (b) V_p at the focal perianastomotic area in the CHS group decreased in the postoperative period and at discharge as compared with baseline; and (c) Unlike in the CHS group, CBF and V_p did not change significantly among the three time points in controls.

In chronic cerebrovascular steno-occlusive diseases such as MMD and atherosclerotic vasculopathy, chronic ischemia is known to trigger the development of abnormal collateral vessels from the extracranial and intracranial arteries.[26,27] Newly-formed collaterals as well as intrinsic intracranial vessels are characterized by impaired cerebral autoregulation.[26,27] Such impaired vessels are thought to be unable to spontaneously constrict in response to a sudden increase in CBF immediately after direct bypass surgery, thus resulting in transient cerebral hyperperfusion until the autoregulation is recovered, as demonstrated by the increase in both absolute and normalized $CBF_{(focal)}$ in the postoperative period and the decrease at discharge in the CHS group. Of note, transient asymptomatic cerebral hyperperfusion was noted in nonoperated hemispheres, which might have been attributed to the presence of circulatory anastomosis and bilateral communication (i.e., circle of Willis) and the presence of global autoregulatory dysfunction.

DCE technique dynamically images the leakage of gadolinium-based contrast agent from the blood plasma to extravascular extracellular space in the brain through the BBB, which serves as a filter. In various pathological conditions with BBB injury, the distribution of gadolinium across the BBB is different from that in normal brain tissue.[8,10–13,28]

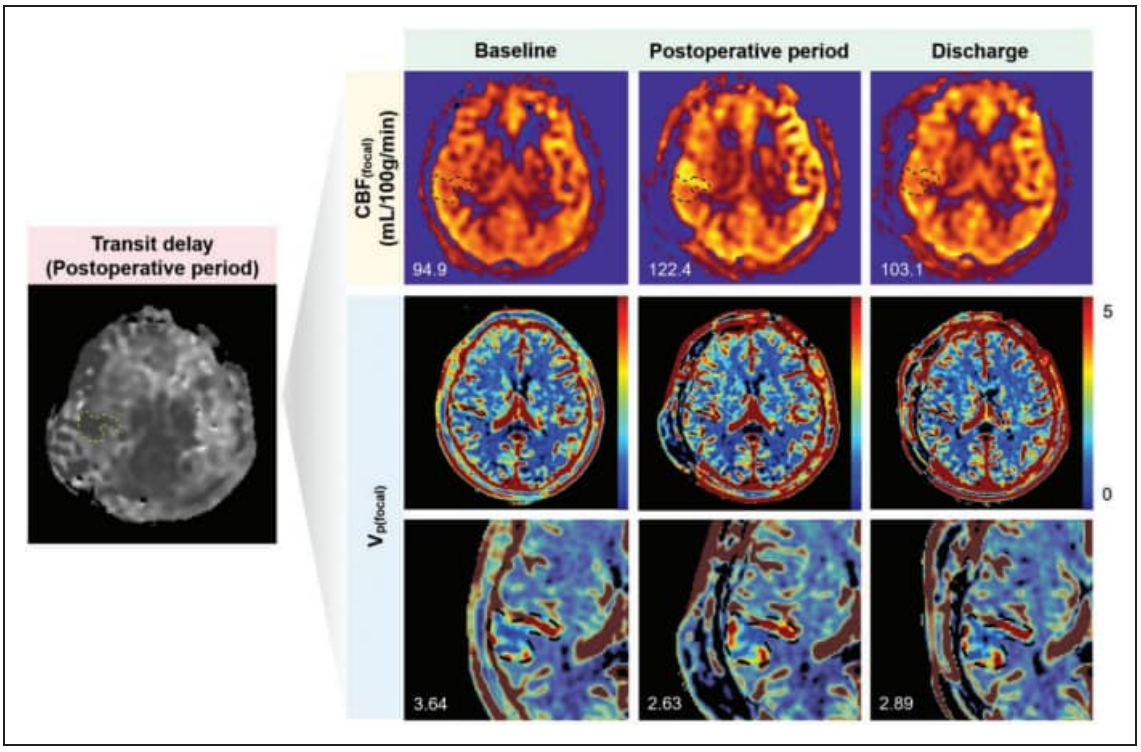

Figure 2. Transit delay, $CBF_{(focal)}$, and $V_{p(focal)}$ maps of a 60-year-old woman with symptoms suggestive of CHS. Dotted lines represent the focal perianastomotic area. Numbers in the lower left corner represent CBF and V_p values in the focal perianastomotic area. When deriving the value of each parameter, the upper and lower 5% values were trimmed to exclude outliers. In this case, $CBF_{(focal)}$ increases in the postoperative period and decreases at discharge. $V_{p(focal)}$ decreases in the postoperative period, especially in the cortex of the anterior portion of the focal mask, and remains decreased at discharge. $CBF_{(focal)}$, cerebral blood flow in the focal perianastomotic area; CHS, cerebral hyperperfusion syndrome; $V_{p(focal)}$, fractional plasma volume in the focal perianastomotic area.

Various DCE MR pharmacokinetic models can be used to calculate the difference in gadolinium distribution due to the change in BBB permeability, which are represented by quantitative variables such as K^{trans} (i.e., volume transfer constant between the plasma and extravascular extracellular space), V_e (i.e., fractional interstitial volume), and V_p (i.e., fractional plasma volume).[7,29,30] Among the various quantitative DCE-MRI parameters, K^{trans} and V_e are thought to be more direct measures of BBB permeability. Under the circumstances of mild BBB disruption with negligible back-diffusion, the Patlak model is considered more appropriate for the measurement of low BBB permeability because the extended Tofts model, which takes into account back-diffusion, can cause overfitting.[7,9,29–31] However, using the Patlak model, we can only calculate K^{trans} and V_p but not V_e. The fact that V_p at the focal perianastomotic area in CHS group decreased in the postoperative period despite the increase in CBF implies that the decrease in V_p may reflect BBB impairment in patients with CHS. Previous studies on migraine and mild TBI have demonstrated that V_p may reflect BBB integrity in CNS pathology with subtle BBB disruption.[9,31]

A Yu J et al's meta-analysis, including 27 cohort studies, reported that the most common CHS-related problem was a transient neurologic deficit (70.2%).[32] Transient neurologic deficits included aphasia, headache, hemiparesis and facial palsy, explained as transient dysfunction due to local hyperperfusion and focal cerebral edema. In our study, the most common symptoms were motor dysphasia, sensory disturbance, motor weakness, and dysarthria. This finding is considered to be attributed to the locations of anastomosis around the functioning cortices. Although ideal selection of the target recipient arteries remains debatable, supra-sylvian cortical branches are generally selected as recipients.[33] Therefore, clinical presentations in the CHS group are likely to correspond to the hyperperfused areas close to the anastomosis sites. Usually, two to three symptoms developed and improved sequentially, which might be explained by the sequential change in cortical areas with neuronal dysfunction.

At discharge, symptoms nearly improved and CBF was stabilized, but V_p remained low relative to the baseline. Previous studies have reported that angiogenic factors and extracellular matrix proteins are overexpressed in long-term cortical ischemia in MMD and

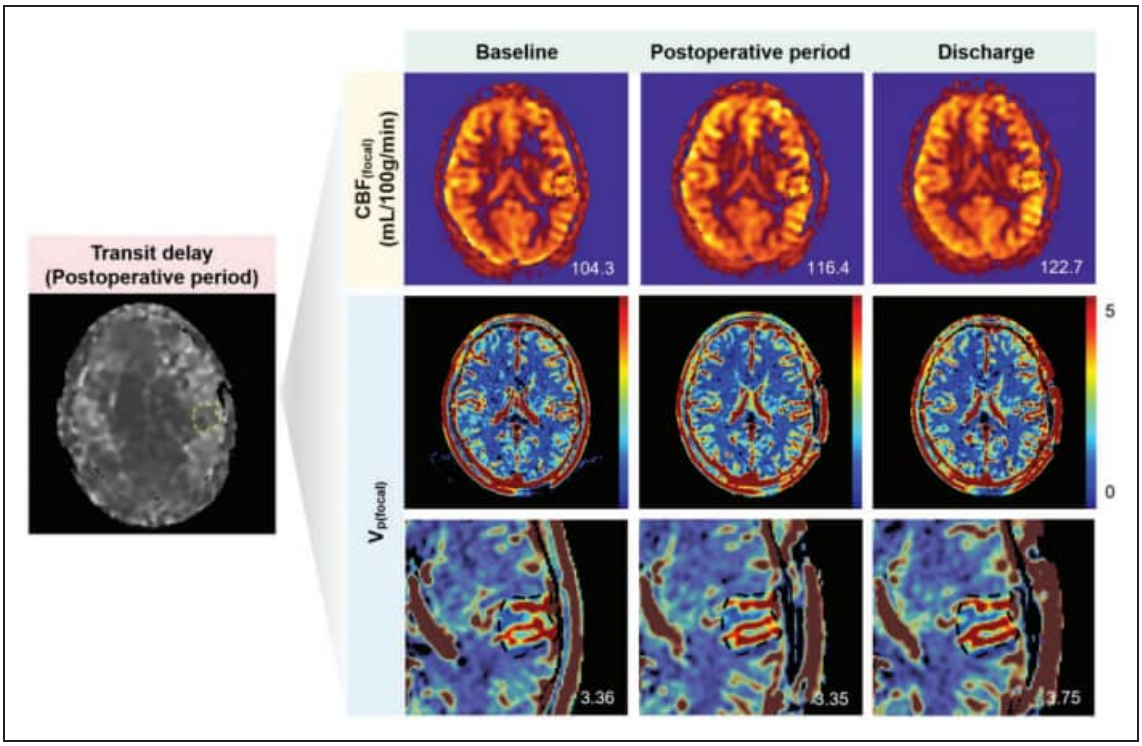

Figure 3. Transit delay, $CBF_{(focal)}$, and $V_{p(focal)}$ maps of a 37-year-old woman in the control group. Dotted lines represent the focal perianastomotic area. Numbers in the lower right corner represent CBF and V_p values in the focal anastomosis area. When deriving the value of each parameter, the upper and lower 5% values were trimmed to exclude outliers. In this case, $CBF_{(focal)}$ slightly increases in the postoperative period and at discharge. $V_{p(focal)}$ does not differ significantly among the three time points. $CBF_{(focal)}$, cerebral blood flow in the focal perianastomotic area; CHS, cerebral hyperperfusion syndrome; $V_{p(focal)}$, fractional plasma volume in the focal perianastomotic area.

trigger neovascularization and an increase in BBB permeability.[34–36] Subsequent increases in nitric oxide expression and free radical production during reperfusion have been reported to cause vasodilation and further increase BBB permeability, ultimately leading to CHS.[37] We speculated that the CBF decrease would lead to the decrease in free radical production, which, in addition to the activation of the reactive oxygen species scavenger system, decreases the oxidative stress stimuli to less than the threshold of neuronal dysfunction, resulting in symptom improvement. V_p, on the other hand, might have been maintained low longer because of residual free radicals, despite the decreased free radical production and increased activity of the reactive oxygen species scavenger system.

Careful monitoring and proper control of blood pressure are the key components in the preventive and treatment strategies for CHS, while the use of drugs, such as antioxidants, free radical scavengers, hypertonic saline, and mannitol, may be considered in select cases, despite the low clinical evidences.[38] Recently, pretreatment with the free radical scavenger edaravone has been shown to reduce the occurrence of hyperperfusion after carotid endarterectomy and CHS-related transient neurological deficits in MMD.[39,40] In addition, Fujimura et al. have reported that minocycline prevents focal neurological deficits due to CHS after bypass for MMD by blocking matrix metalloproteinase, which contributes to edema formation and hemorrhagic conversion following cerebral ischemia-reperfusion.[41] Yet, the effects of minocycline and edaravone seem unsatisfactory and unavailable in some countries. Based on our results in patients inspired from the animal experiment first reporting the association between BBB disruption and CHS,[6] BBB-stabilizing drugs may be a useful adjunct to other strategies to prevent and treat the CHS.

Our study has a few limitations. First, owing to the retrospective nature of this study, there could have been selection bias. Second, our total acquisition time for DCE-MRI was relatively short. Detecting subtle changes in BBB permeability requires relatively long measurements so that more contrast agents can enter the extravascular space. However, the relatively short acquisition time was partly overcome by the use of gadobutrol with relatively high T1 relaxivity and the

Patlak model. Third, this is single center study and the sample size was relatively small. Thus a further prospective study with a larger sample size is needed for validation and generalization. Fourth, at discharge, most of the patients in the CHS group had some residual symptoms despite considerable recovery, and thus complete recovery of BBB permeability to the preoperative level could not be confirm in this study. A future study with a larger study population and a longer follow-up period is warranted to validate the finding. Fifth, despite the change in V_p, we found no significant difference in K^{trans} between the CHS and control groups. This might be partly attributable to the fact that K^{trans} values were very small and had lower reproducibility than V_p values.

In conclusion, an increase in CBF and a decrease in V_p were observed at the focal perianastomotic areas in patients with CHS after bypass surgery for cerebrovascular steno-occlusive diseases. Preclinical observations that BBB disruption may be implicated in the development of CHS were confirmed in the human brain using noninvasive DCE-MRI. Further prospective studies with larger numbers of participants and longer DCE-MRI acquisition times are warranted for validation.

Funding

This work was supported by the National Research Foundation of Korea (NRF) grant funded by the Korea government (MSIT) (NRF-2021R1A4A1028713 and NRF-2023R1A2C3003250). This study was supported by grant no. 0420213080 and 0320230270 from the SNUH Research Fund.

Declaration of conflicting interests

The author(s) declared no potential conflicts of interest with respect to the research, authorship, and/or publication of this article.

Authors' contributions

R.E.Y. and W.S.C. contributed to the conception and design of the study, acquisition and analysis of data, and drafting a significant portion of the manuscript or figures. K.L. contributed to acquisition and analysis of data and drafting a significant portion of the manuscript or figures. S.H.C., S.H.L., K. M.K., H.S.K., and J.E.K. contributed to acquisition and analysis of data.

Supplementary material

Supplemental material for this article is available online.

References

1. Lin YH and Liu HM. Update on cerebral hyperperfusion syndrome. *J Neurointerv Surg* 2020; 12: 788–793.
2. van Mook WN, Rennenberg RJ, Schurink GW, et al. Cerebral hyperperfusion syndrome. *Lancet Neurol* 2005; 4: 877–888.
3. Huibers AE, Westerink J, de Vries EE, et al. Editor's choice – cerebral hyperperfusion syndrome after carotid artery stenting: a systematic review and meta-analysis. *Eur J Vasc Endovasc Surg* 2018; 56: 322–333.
4. Fujimura M, Shimizu H, Inoue T, et al. Significance of focal cerebral hyperperfusion as a cause of transient neurologic deterioration after extracranial-intracranial bypass for moyamoya disease: comparative study with non-moyamoya patients using N-isopropyl-p-[(123)I] iodoamphetamine single-photon emission computed tomography. *Neurosurgery* 2011; 68: 957–964. discussion 964–955.
5. Uchino H, Kuroda S, Hirata K, et al. Predictors and clinical features of postoperative hyperperfusion after surgical revascularization for moyamoya disease: a serial single photon emission CT/positron emission tomography study. *Stroke* 2012; 43: 2610–2616.
6. Mansour A, Rashad S, Niizuma K, et al. A novel model of cerebral hyperperfusion with blood-brain barrier breakdown, white matter injury, and cognitive dysfunction. *J Neurosurg* 2019; 133: 1460–1472.
7. Heye AK, Culling RD, Valdes HMC, et al. Assessment of blood-brain barrier disruption using dynamic contrast-enhanced MRI. A systematic review. *Neuroimage Clin* 2014; 6: 262–274.
8. Ingrisch M, Sourbron S, Morhard D, et al. Quantification of perfusion and permeability in multiple sclerosis: dynamic contrast-enhanced MRI in 3D at 3T. *Invest Radiol* 2012; 47: 252–258.
9. Kim YS, Kim M, Choi SH, et al. Altered vascular permeability in migraine-associated brain regions: Evaluation with dynamic contrast-enhanced MRI. *Radiology* 2019; 292: 713–720.
10. Raja R, Rosenberg GA and Caprihan A. MRI measurements of Blood-Brain barrier function in dementia: a review of recent studies. *Neuropharmacology* 2018; 134: 259–271.
11. Thrippleton MJ, Backes WH, Sourbron S, et al. Quantifying blood-brain barrier leakage in small vessel disease: Review and consensus recommendations. *Alzheimers Dement* 2019; 15: 840–858.
12. van de Haar HJ, Burgmans S, Jansen JF, et al. Blood-Brain barrier leakage in patients with early alzheimer disease. *Radiology* 2016; 281: 527–535.
13. Yoo RE, Choi SH, Oh BM, et al. Quantitative dynamic contrast-enhanced MR imaging shows widespread blood-brain barrier disruption in mild traumatic brain injury patients with post-concussion syndrome. *Eur Radiol* 2019; 29: 1308–1317.
14. Ferre JC, Bannier E, Raoult H, et al. Arterial spin labeling (ASL) perfusion: techniques and clinical use. *Diagn Interv Imaging* 2013; 94: 1211–1223.
15. Noguchi T, Yoshiura T, Hiwatashi A, et al. Perfusion imaging of brain tumors using arterial spin-labeling: correlation with histopathologic vascular density. *AJNR Am J Neuroradiol* 2008; 29: 688–693.
16. Blauwblomme T, Naggara O, Brunelle F, et al. Arterial spin labeling magnetic resonance imaging: toward noninvasive diagnosis and follow-up of pediatric brain

arteriovenous malformations. *J Neurosurg Pediatr* 2015; 15: 451–458.
17. Heit JJ, Thakur NH, Iv M, et al. Arterial-spin labeling MRI identifies residual cerebral arteriovenous malformation following stereotactic radiosurgery treatment. *J Neuroradiol* 2020; 47: 13–19.
18. Yoo RE, Yun TJ, Yoon BW, et al. Identification of cerebral perfusion using arterial spin labeling in patients with seizures in acute settings. *PLoS One* 2017; 12: e0173538.
19. Sakaki T, Tsujimoto S, Nishitani M, et al. Perfusion pressure breakthrough threshold of cerebral autoregulation in the chronically ischemic brain: an experimental study in cats. *J Neurosurg* 1992; 76: 478–485.
20. Jia B, Xiao W and Wang TL. [Expression and mechanism of nitric oxide synthase in cerebral hyperperfusion rats]. *Zhonghua Yi Xue Za Zhi* 2016; 96: 468–471.
21. von Elm E, Altman DG, Egger M, et al. The strengthening the reporting of observational studies in epidemiology (STROBE) statement: guidelines for reporting observational studies. *Lancet* 2007; 370: 1453–1457.
22. Cho WS, Kim JE, Kim CH, et al. Long-term outcomes after combined revascularization surgery in adult moyamoya disease. *Stroke* 2014; 45: 3025–3031.
23. Kim JE, Oh CW, Kwon OK, et al. Transient hyperperfusion after superficial temporal artery/middle cerebral artery bypass surgery as a possible cause of postoperative transient neurological deterioration. *Cerebrovasc Dis* 2008; 25: 580–586.
24. Barber PA, Demchuk AM, Zhang J, et al. Validity and reliability of a quantitative computed tomography score in predicting outcome of hyperacute stroke before thrombolytic therapy. ASPECTS study group. Alberta stroke programme early CT score. *Lancet* 2000; 355: 1670–1674.
25. Ivens S, Gabriel S, Greenberg G, et al. Blood-brain barrier breakdown as a novel mechanism underlying cerebral hyperperfusion syndrome. *J Neurol* 2010; 257: 615–620.
26. Hayashi K, Horie N, Suyama K, et al. Incidence and clinical features of symptomatic cerebral hyperperfusion syndrome after vascular reconstruction. *World Neurosurg* 2012; 78: 447–454.
27. Zhao WG, Luo Q, Jia JB, et al. Cerebral hyperperfusion syndrome after revascularization surgery in patients with moyamoya disease. *Br J Neurosurg* 2013; 27: 321–325.
28. Kim JY, Yoon MJ, Park JE, et al. Radiomics in peritumoral non-enhancing regions: fractional anisotropy and cerebral blood volume improve prediction of local progression and overall survival in patients with glioblastoma. *Neuroradiology* 2019; 61: 1261–1272.
29. Cramer SP and Larsson HB. Accurate determination of blood-brain barrier permeability using dynamic contrast-enhanced T1-weighted MRI: a simulation and in vivo study on healthy subjects and multiple sclerosis patients. *J Cereb Blood Flow Metab* 2014; 34: 1655–1665.
30. Heye AK, Thrippleton MJ, Armitage PA, et al. Tracer kinetic modelling for DCE-MRI quantification of subtle blood-brain barrier permeability. *Neuroimage* 2016; 125: 446–455.
31. Yoen H, Yoo RE, Choi SH, et al. Blood-brain barrier disruption in mild traumatic brain injury patients with post-concussion syndrome: evaluation with region-based quantification of dynamic contrast-enhanced MR imaging parameters using automatic whole-brain segmentation. *Korean J Radiol* 2021; 22: 118–130.
32. Yu J, Zhang J, Li J, et al. Cerebral hyperperfusion syndrome after revascularization surgery in patients with moyamoya disease: systematic review and meta-analysis. *World Neurosurg* 2020; 135: 357–366 e354.
33. Zhang J, Li S, Fujimura M, et al. Hemodynamic analysis of the recipient parasylvian cortical arteries for predicting postoperative hyperperfusion during STA-MCA bypass in adult patients with moyamoya disease. *J Neurosurg* 2019; 134: 17–24.
34. Fujimura M, Gasche Y, Morita-Fujimura Y, et al. Early appearance of activated matrix metalloproteinase-9 and blood-brain barrier disruption in mice after focal cerebral ischemia and reperfusion. *Brain Res* 1999; 842: 92–100.
35. Fujimura M, Kaneta T, Mugikura S, et al. Temporary neurologic deterioration due to cerebral hyperperfusion after superficial temporal artery-middle cerebral artery anastomosis in patients with adult-onset moyamoya disease. *Surg Neurol* 2007; 67: 273–282.
36. Narducci A, Yasuyuki K, Onken J, et al. In vivo demonstration of blood-brain barrier impairment in moyamoya disease. *Acta Neurochir (Wien)* 2019; 161: 371–378.
37. Janigro D, West GA, Nguyen TS, et al. Regulation of blood-brain barrier endothelial cells by nitric oxide. *Circ Res* 1994; 75: 528–538.
38. Farooq MU, Goshgarian C, Min J, et al. Pathophysiology and management of reperfusion injury and hyperperfusion syndrome after carotid endarterectomy and carotid artery stenting. *Exp Transl Stroke Med* 2016; 8: 7.
39. Ogasawara K, Inoue T, Kobayashi M, et al. Pretreatment with the free radical scavenger edaravone prevents cerebral hyperperfusion after carotid endarterectomy. *Neurosurgery* 2004; 55: 1060–1067.
40. Uchino H, Nakayama N, Kazumata K, et al. Edaravone reduces hyperperfusion-related neurological deficits in adult moyamoya disease: historical control study. *Stroke* 2016; 47: 1930–1932.
41. Fujimura M, Niizuma K, Inoue T, et al. Minocycline prevents focal neurological deterioration due to cerebral hyperperfusion after extracranial-intracranial bypass for moyamoya disease. *Neurosurgery* 2014; 74: 163–170; discussion 170.